Effect of pressure on the phase diagram of binary mixtures of n-alkanes

Chitoshi Nakafuku* and Takeshi Sugiuchi
Faculty of Education, Kochi University, Kochi 780, Japan
(Received 18 November 1992; revised 25 February 1993)

The effect of pressure on the phase diagram of n-triacontane (C_{30})/n-docosane (C_{22}) binary mixture and n-triacontane (C_{30})/n-hexacosane (C_{26}) binary mixture was studied up to 500 MPa by high-pressure differential thermal analysis. The C_{30}/C_{22} mixture at 0.1 MPa has a eutectic-type phase diagram, with the hexagonal phase appearing just below the melting temperature on the C_{30} side. The eutectic temperature, T_e, is 45.1°C and the eutectic composition lies between 15 and 20 wt% C_{30}. The hexagonal phase and the low-temperature transition disappear above 100 MPa. The change of the phase diagram with pressure was interpreted by the different pressure dependence of the melting temperature, T_m, of C_{30} and C_{22} and that of T_e. Pressure dependence of T_e was 0.247 K MPa^{-1}, which is smaller than that of C_{22} (0.279 K MPa^{-1}) and C_{30} (0.276 K MPa^{-1}). The C_{30}/C_{26} mixture has a solid-solution-type phase diagram, showing an almost linear melting curve from the T_m of C_{30} to the T_m of C_{22}, and the lower critical transition temperature on the hexagonal transition curve at 0.1 MPa. At elevated pressure, the melting curve changes to become downwardly convex and the transition curve moves close to the melting curve.

(Keywords: binary mixture; phase diagram; eutectic melting)

INTRODUCTION

In some binary mixtures containing crystalline polymers, a eutectic-type phase diagram is observed[1–4]. The effect of pressure on the eutectic phase diagram of binary mixtures of crystalline polymers with high-melting-temperature diluents (HMTD) has been studied[5,6]. In these mixtures, including polyethylene (PE) as the crystalline polymer, the phase diagram changed with pressure, i.e. the difference between the melting temperature (T_m) of HMTD and the eutectic temperature (T_e) increased with pressure in the hypo-eutectic region on the weight fraction of PE; however, the difference between T_m of PE and T_e decreased with pressure in the hyper-eutectic region.

The phase diagram of the binary mixture of n-alkanes has been studied by several authors[7–12]. The type of phase diagram depends on the carbon number of the component n-alkanes. According to Nechitailo *et al.*[7], the phase diagram of the C_{30}/C_{22} mixture is eutectic; T_e is about 46°C and the eutectic point occurs at about 15 wt% C_{30} (i.e. weight fraction of C_{30}, $W_{C30} = 0.3$). The region of the hexagonal phase appears near the T_m of C_{30}. The binary mixture of C_{30} and C_{26} has a solid-solution-type phase diagram. In this case, T_m and the hexagonal transition temperature (T_h) change continuously between the T_ms of the component alkane with different weight fractions.

The T_m of a polymer crystal is greatly affected by the application of pressure because the intermolecular force between the molecular chains is weak. The T_m of n-alkanes with CH_2 chains also changes with pressure. The pressure dependence of T_m and T_h of some pure n-alkanes with odd carbon numbers has been reported[13,14]. In all alkanes, the hexagonal transition curve moves close to the melting curve of the hexagonal phase with increasing pressure; the triple point of the transition curve, melting curve of the hexagonal phase and the melting curve of the crystal phase exists between about 150 and 300 MPa, depending on the molecular length. It has been reported[15] that in C_{22}, the triple point exists at about 50 MPa. The phase diagram of the binary mixture of n-alkanes composed of chain molecules is expected to change greatly with pressure.

In this paper, the effect of pressure on the phase diagram of two binary mixtures of n-alkanes is studied. In the n-alkanes with odd carbon number, some phase transitions appear below T_m and the melting behaviour is complicated[14,16]. However, n-alkanes with even carbon number above C_{22}, as used in this study, show a T_h only just below T_m[17]. High-pressure differential thermal analysis (d.t.a.) was performed up to 500 MPa on the two binary mixtures with different weight fractions: the C_{30}/C_{22} mixture showed a eutectic-type phase diagram, and the C_{30}/C_{26} mixture showed a solid-solution-type phase diagram at atmospheric pressure. X-ray diffraction measurements were performed on the binary mixtures at elevated temperature to study the mechanism of phase changes at atmospheric pressure.

* To whom correspondence should be addressed

0032-3861/93/234945-08

EXPERIMENTAL

The samples (C_{30}, C_{22} and C_{26}) used in this study were purchased from Sigma Chemical Co. The purity of all the samples was approximately 99%.

Powder samples of the two n-alkanes were mixed in the desired weight ratio and melted at 100°C for 10 min in a glass tube (i.d. 1.8 mm). After cooling to room temperature at a rate of 1.2 K min^{-1}, a rod-like sample was obtained.

The high-pressure d.t.a. apparatus used in this study has been described elsewhere[18]. A small sample cut from the rod was tightly covered with aluminium foil and attached with epoxy resin to the thermocouple junction of the high-pressure d.t.a. apparatus. The high-pressure d.t.a. was performed after keeping the sample for more than 5 min at a desired pressure. The heating rate of the melting process was 6 K min^{-1}. After reaching a temperature about 15°C higher than the peak T_m, the sample was cooled. The cooling rate was not controlled, and varied from about 5 K min^{-1} at high temperature to about 1 K min^{-1} at low temperature.

The temperature change of the wide-angle X-ray diffraction (WAXD) pattern of the mixture was measured up to 70°C using a home-made heating device on the diffractometer. The sample temperature was detected by an alumel–chromel thermocouple junction attached to the foil-covered sample. CuKα radiation was used as an incident X-ray beam.

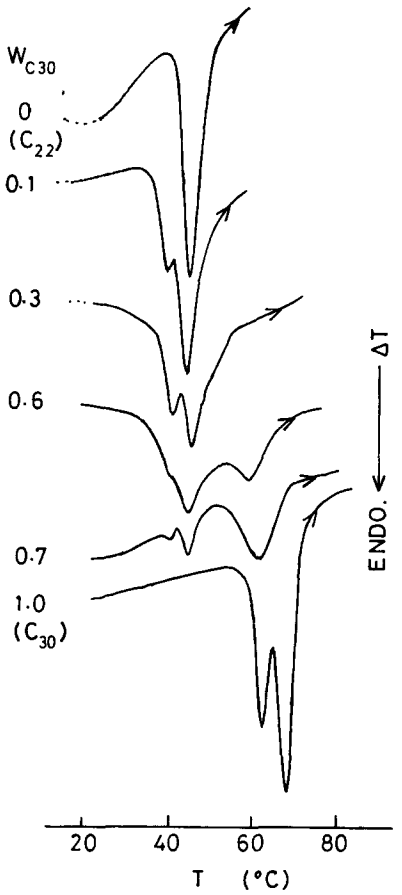

Figure 1 D.t.a. melting curve at atmospheric pressure of C_{30}/C_{22} binary mixture. Peak temperatures are drawn in the figure

RESULTS AND DISCUSSION

Phase diagram of C_{30}/C_{22} binary mixture

Figure 1 shows the change of the d.t.a. melting curve at 0.1 MPa for C_{30}/C_{22} mixtures with different values of W_{C30}. A very small shoulder appears on the low-temperature side of the main peak for pure C_{22}. When $W_{C30}=0.1$, a small peak appears on the lower-temperature side due to a phase transition in the mixture. The curve is complicated above $W_{C30}=0.3$ because of the appearance of endothermic peaks due to the phase transition, the eutectic melting and the melting of C_{30}.

Figure 2 shows the effect of pressure on the d.t.a. melting and crystallization curves of pure C_{30}. At atmospheric pressure, two endothermic peaks in the heating process and two exothermic peaks in the cooling process appear. The low-temperature peak is due to the phase transition from the monoclinic to the hexagonal crystal system, and the high-temperature peak is due to the melting of the hexagonal phase. The intensity of the low-temperature peak decreases and the peak moves close to the high-temperature peak with pressure; the peak disappears above 100 MPa. This indicates that the hexagonal phase does not exist above 100 MPa in C_{30}. The pressure of the triple point of C_{30}, determined by precise measurement at intervals of 20 MPa in the high-pressure d.t.a., was between 80 and 100 MPa. This is very close to the pressure of the triple point (about 80 MPa) of C_{24} (ref. 13). In the crystallization process, the hexagonal transition disappears above 300 MPa.

Figure 3 shows the effect of pressure on the d.t.a. melting and crystallization curves of pure C_{22}. In this sample, a very small shoulder due to the hexagonal transition appears on the low-temperature side of the main peak in the d.t.a. curve of melting at 0.1 MPa, but a single endothermic peak is observed from 50 to 500 MPa.

Figure 4 shows the effect of pressure on the d.t.a. melting and crystallization curves of the C_{30}/C_{22} mixture with $W_{C30}=0.3$. Three endothermic peaks appear in the melting process at 0.1 MPa. The high-temperature peak is due to the melting of C_{30} and the medium-temperature peak is due to the eutectic melting. These peaks shifted to the high-temperature side with pressure. According to Nechitailo *et al.*[7], the low-temperature peak, which appears only in the mixture, is due to the phase transition from the α-form to the γ-modification. This peak decreased in intensity with pressure and disappeared completely above 100 MPa. An exothermic peak on the low-temperature side clearly appears in the crystallization process up to 100 MPa, though the endothermic peak on the low-temperature side in the melting process disappears at 100 MPa. This may be due to the difference between the heating rate and the cooling rate. In the cooling process, the cooling rate could not be controlled and it changed as described in the Experimental section.

To determine the origin of this transition, the effect of temperature on the WAXD pattern of the mixture was studied up to 70°C (above T_m of the sample). *Figure 5* shows the effect of temperature on the WAXD pattern of the mixture with $W_{C30}=0.5$. At 20°C, diffraction peaks from the triclinic crystal of C_{22} and the monoclinic crystal of C_{30} are observed. In the heating process, only the diffraction peak from the monoclinic crystal is observed at 43°C, which is above the transition temperature and below the eutectic melting temperature. At 52°C, i.e.

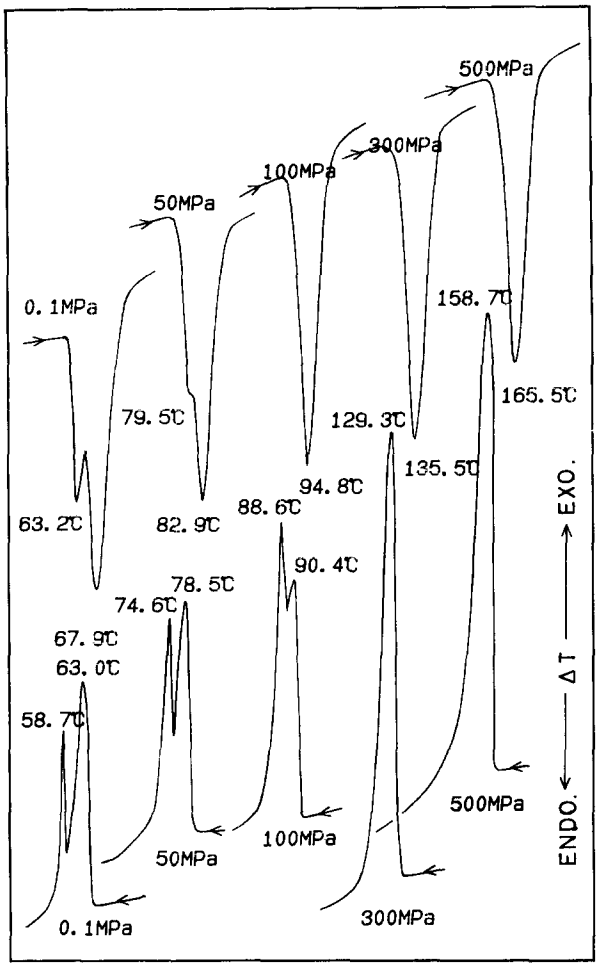

Figure 2 Effect of pressure on the d.t.a. melting and crystallization curves of pure C_{30}

between the eutectic melting and C_{30} melting, the intensity of the diffraction peak decreased and the peak disappeared above the melting temperature. Therefore, this transition is the solid–solid transition from triclinic to monoclinic structure of the C_{22} crystal.

Figure 6 shows the pressure dependence of the endothermic peak temperatures of the melting of pure C_{30} and C_{22} and the melting and eutectic melting of C_{30} and C_{22} in the binary mixture with $W_{C30}=0.3$. It is observed in the figure that the inclination of the curve of T_e is smaller than that of T_m of C_{30} and C_{22}.

To determine the pressure dependence of T_m of pure C_{30} and C_{22} and T_m of C_{30} and C_{22} in mixtures with different weight fractions, the curve is fitted to a quadratic equation of the form $T_m = A + BP - CP^2$, where P is the pressure. The values of coefficients A, B and C for pure C_{30}, C_{30} in the mixture, pure C_{22} and C_{22} in the mixture are summarized in *Table 1*. The pressure dependence of T_m of C_{30} (0.276 K MPa^{-1}) is slightly smaller than that of PE (0.28 ~ 0.30 K MPa^{-1})[6,19] with the same molecular structure. *Table 2* lists the values of coefficients A, B and C for T_e determined by the same method for the quadratic equation of the C_{30}/C_{22} mixture. The average value of the pressure dependence of T_e is 0.247 K MPa^{-1}, which is smaller than that of T_m of C_{30} and C_{22}.

To draw the phase diagram of the binary mixture at a desired pressure, values of T_m and T_e at the pressure were determined by calculation using the above equation and the values given in *Tables 1* and *2*. The transition temperature T_t and T_h were determined by using the d.t.a. data independently. *Figures 7a–c* show the effect of pressure on the phase diagram. The phase diagram at 0.1 MPa in this study resembles the phase diagram of the C_{30}/C_{22} mixture reported by Nechitailo *et al.*[7], but the triple point of the melting curve of C_{30} and the hexagonal transition curve in this study exists at $W_{C30} \approx 0.8$, which is slightly larger than the position of the triple point reported by them. This difference may be due to the difference in the samples used. The low-temperature transition in the mixture exists in the range $W_{C30} = 0.05$–0.8 but it does not appear above 100 MPa. Under high pressure, the molecular motion of C_{30} and C_{22} is hindered and the eutectic melting occurs directly with increasing molecular motion in the heating process without transition.

The hexagonal phase of C_{30} disappears below $W_{C30}=0.8$ at 0.1 MPa. The C_{30} crystals melt before the hexagonal transition occurs owing to the solvent effect of molten C_{22} in the mixture. Under high pressure, above 100 MPa, the molecular motion of C_{30} is hindered by the decreased intermolecular distance and it should melt without hexagonal transition. This is deduced from the fact that in PE with the same molecular structure, no hexagonal phase appears below the melting temperature at 0.1 MPa, although the orthorhombic crystal structure approaches the hexagonal structure owing to the different thermal expansion between the a and b axes in the unit cell. In the hexagonal phase, the ratio of the a axis to the b axis

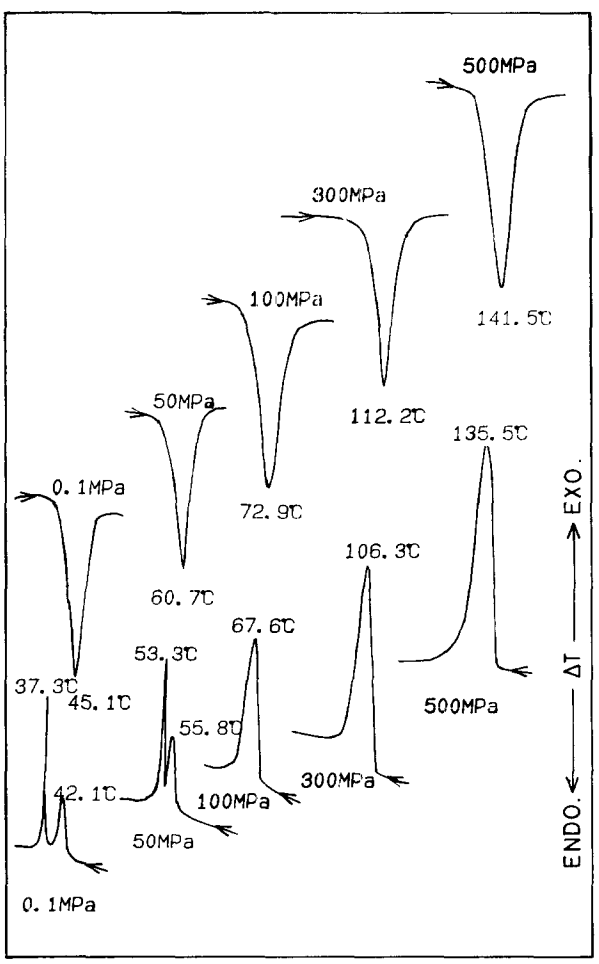

Figure 3 Effect of pressure on the d.t.a. melting and crystallization curves of pure C_{22}

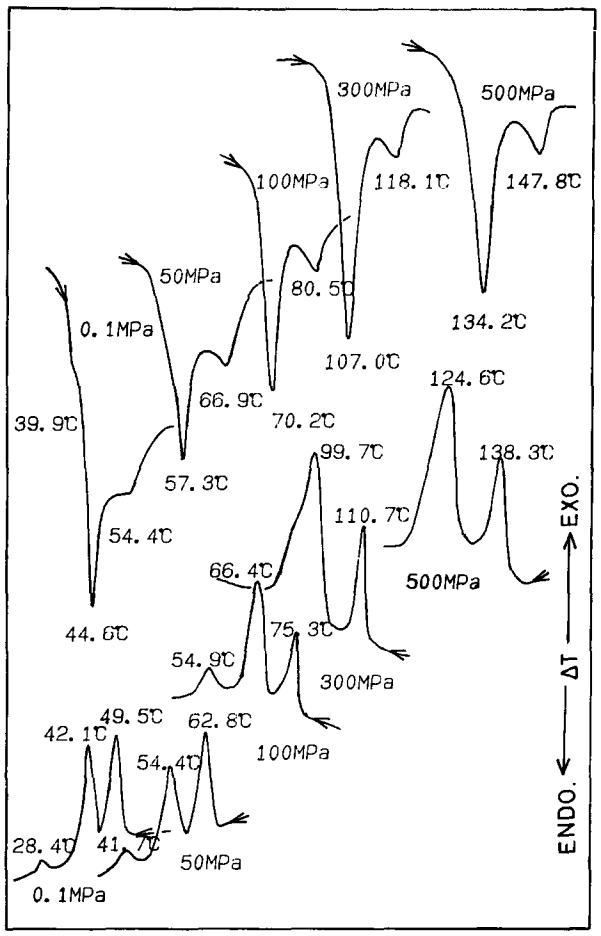

Figure 4 Effect of pressure on the d.t.a. melting and crystallization curves of the C_{30}/C_{22} mixture with $W_{C30}=0.3$

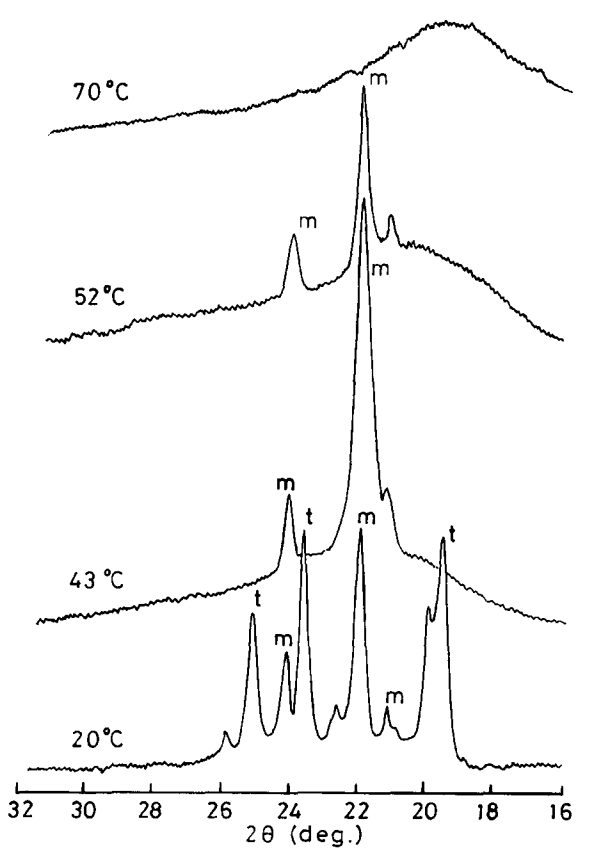

Figure 5 WAXD pattern of the C_{30}/C_{22} mixture with $W_{C30}=0.5$, at various temperatures. t and m represent the diffraction peak from triclinic crystal and monoclinic crystal, respectively

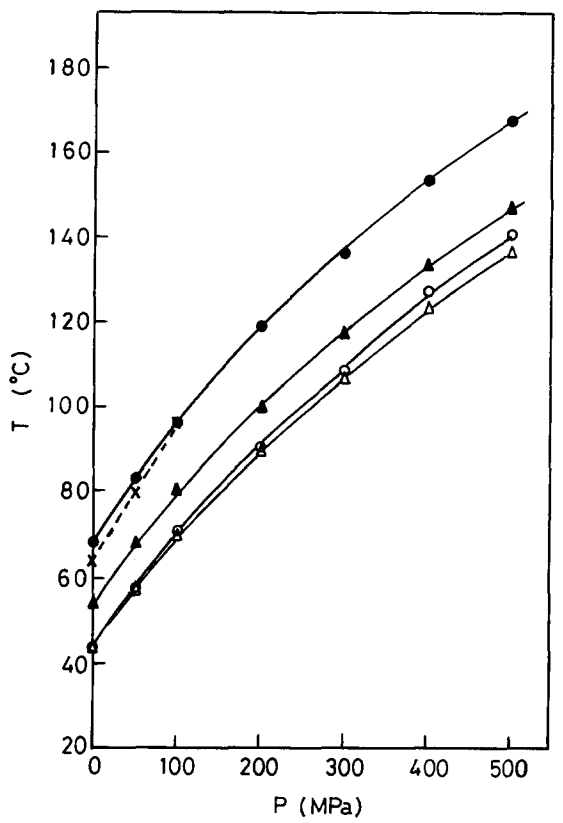

Figure 6 Pressure dependence of T_m of pure C_{30}, pure C_{22} and T_m of C_{30} and T_e in the mixture with $W_{C30}=0.3$. ●, T_m of pure C_{30}; -- × --, hexagonal transition of C_{30}; ○, T_m of pure C_{22}; △, T_m of C_{30} in $W_{C30}=0.3$; ▲, eutectic melting temperature in $W_{C30}=0.3$

Table 1 Values of A, B and C in the equation $T_m=A+BP-CP^2$, for the melting temperature of C_{30} ($W_{C30}=1.0$–0.2) and C_{22} ($W_{C30}=0.15$–0.0) in the mixture for different weight fractions in d.t.a. up to 500 MPa

W_{C30}	A (°C)	B ($\times 10^{-1}$ K MPa^{-1})	C ($\times 10^{-4}$ K MPa^{-2})
1.0(C_{30})	68.3	2.76	1.645
0.95	67.2	2.73	1.617
0.9	66.0	2.70	1.567
0.8	62.7	2.84	1.765
0.7	61.8	2.88	1.865
0.6	58.7	2.71	1.581
0.5	56.8	2.81	1.782
0.4	54.7	2.79	1.824
0.3	53.7	2.64	1.556
0.25	52.3	2.58	1.492
0.2	45.5	2.59	1.462
0.15	46.4	2.74	1.759
0.1	46.4	2.75	1.792
0.05	45.6	2.64	1.528
0.0(C_{22})	46.4	2.79	1.829

becomes $\sqrt{3}:1=1.73$. Mazee[20] reported that the value of a/b in C_{24} increased with temperature from 1.50 at 20.5°C to 1.63 at 38.3°C.

The distance of the eutectic line and the melting curve of C_{30} in the hyper-eutectic region increased with pressure, as shown in the phase diagram at 500 MPa in *Figure 7c*. This is due to the different pressure dependence of T_m and T_e. The difference between T_m of C_{30} and T_e at 0.1 MPa is about 23°C and the difference at 500 MPa is 29°C. Considering that the eutectic melting occurs

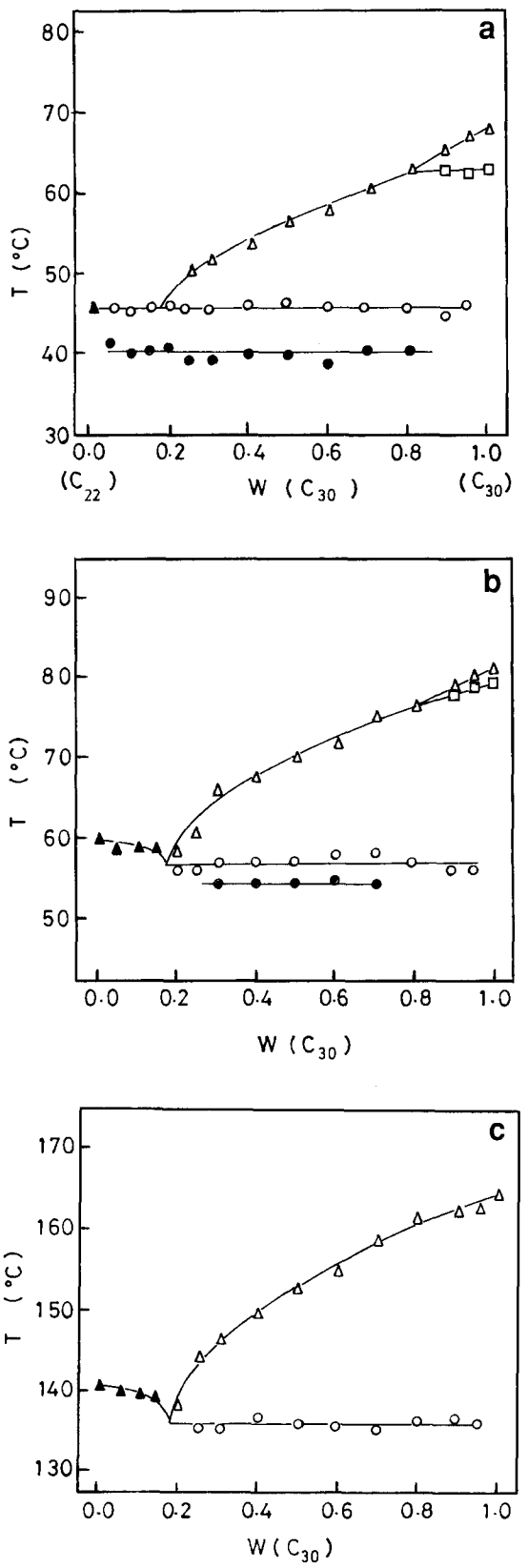

Figure 7 Phase diagram of melting of the C_{30}/C_{22} binary mixture at various pressures: (a) 0.1 MPa; (b) 50 MPa; (c) 500 MPa. ●, Monoclinic transition; ○, eutectic melting; △, melting of C_{30}; ▲, melting of C_{22}; □, hexagonal transition

cooperatively in the increased molecular motion of C_{30} and C_{22} in the heating process, it may reasonably occur at relatively lower temperature than T_m of C_{30} due to the decreased distance of C_{30} and C_{22} under high pressure. The effect of pressure on this binary mixture is different

Table 2 Values of A, B and C in the equation $T_e = A + BP - CP^2$, for the eutectic melting temperature in the binary mixture of C_{30}/C_{22} for different weight fractions in d.t.a. up to 500 MPa. The values of B and C are rounded to two and three decimal places, respectively

W_{C30}	A (°C)	B ($\times 10^{-1}$ K MPa^{-1})	C ($\times 10^{-4}$ K MPa^{-2})
1.0	–	–	–
0.95	–	–	–
0.9	43.7	2.40	1.192
0.8	44.9	2.42	1.206
0.7	46.1	2.47	1.408
0.6	45.3	2.59	1.540
0.5	45.4	2.54	1.457
0.4	46.0	2.42	1.208
0.3	45.1	2.55	1.549
0.25	43.6	2.34	1.454
0.2	–	–	–
0.15	–	–	–
0.1	–	–	–
0.0(C_{22})	–	–	–

from that of PE/HMTD binary mixture[5]. In the PE/HMTD mixture, the difference between T_m of PE and T_e decreased with pressure and the difference between T_m of HMTD and T_c increased with pressure.

In the hypo-eutectic region on C_{30}, the melting curve of C_{22} shifts to the high-temperature side compared to the eutectic melting line with pressure. The endothermic peak of eutectic melting did not appear clearly, but taking into account the small mass of C_{30} in the mixture, the peak of the eutectic melting may be involved in the melting peak of C_{22} in this region. In the cooling process, two exothermic peaks appeared, corresponding to the crystallization of C_{22} and the hexagonal transition between 0.1 and 400 MPa, but the peak due to the eutectic crystallization was not observed clearly in the sample of these weight fractions.

Phase diagram of C_{30}/C_{26} binary mixture

Figure 8 shows the d.t.a. melting curve of the C_{30}/C_{26} binary mixture at 0.1 MPa. The double endothermic peak appears for all the weight fractions and the temperature difference between the high-temperature and low-temperature peak changes depending on the weight fraction.

Figure 9 shows the effect of pressure on the d.t.a. melting and crystallization curves of pure C_{26}. The double endothermic peaks appear in the heating process below 100 MPa. The low-temperature peak is due to the transition from the orthorhombic to the hexagonal crystal and the high temperature peak is due to the melting of the hexagonal crystal. The double exothermic peaks appear in the cooling process, corresponding to the crystallization and hexagonal transition. *Figure 10* shows the pressure dependence of T_m and T_c of pure C_{26}. The triple point of the hexagonal transition curve and the melting curve exists at about 100 MPa, which is very close to the triple point of C_{30}.

Figure 11 shows the effect of pressure on the d.t.a. melting and crystallization curves of the binary mixture with $W_{C30} = 0.5$. Two endothermic peaks in the heating process and two exothermic peaks in the cooling process are observed up to 500 MPa. At room temperature, C_{26} is composed of monoclinic crystals and triclinic crystals. However, the crystal structure in the solid solution of the

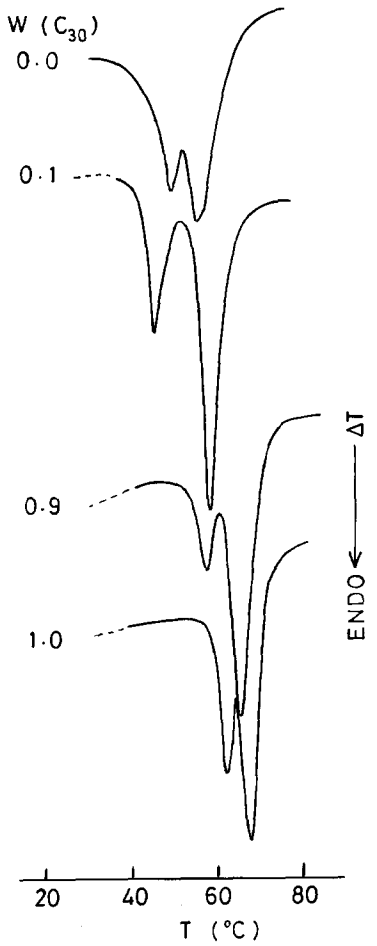

Figure 8 D.t.a. melting curve of the C_{30}/C_{26} binary mixture at 0.1 MPa

Table 3 Values of A, B and C in the equation $T_m = A + BP - CP^2$, for the melting temperature of solid solution of C_{30}/C_{26} for different weight fractions in d.t.a. up to 500 MPa

W_{C30}	A (°C)	B ($\times 10^{-1}$ K MPa^{-1})	C ($\times 10^{-4}$ K MPa^{-2})
1.0	68.3	2.76	1.645
0.9	66.3	2.67	1.487
0.8	66.4	2.53	1.265
0.6	64.7	2.61	1.639
0.5	62.3	2.50	1.473
0.4	62.8	2.58	1.608
0.2	60.2	2.53	1.645
0.1	59.3	2.46	1.419
0.0(C_{26})	58.4	2.65	1.477

mixture at 10°C is orthorhombic, as shown in the X-ray diffraction pattern in *Figure 12*. In *Figure 12*, the diffraction peak from the hexagonal phase is observed at 55°C (the temperature between the two endothermic peaks in d.t.a.) and a broad diffraction pattern from the melt appears at 70°C above T_m. The low-temperature peak in the d.t.a. melting curve is due to the phase transition from the orthorhombic to the hexagonal crystal and the high-temperature peak is due to the melting of the hexagonal crystal.

Figure 13 shows the pressure dependence of T_m and T_h of the solid solution of C_{30} and C_{26} in the mixture with $W_{C30} = 0.6$. The difference between T_m and T_h decreased with pressure. Pressure dependence curves of the melting and the hexagonal transition of the solid solution are fitted to the quadratic equation and the values of coefficients are listed in *Tables 3* and *4*. The pressure dependence of T_h at atmospheric pressure is slightly larger than that of T_m. Values of T_m and T_h under high pressure were determined by the same method used to obtain T_m and T_e of the C_{30}/C_{22} mixture under high pressure.

Figure 14 shows the effect of pressure on the phase diagram of the C_{30}/C_{26} binary mixture. A minimum appears in the hexagonal transition curve at around $W_{C30} = 0.2$ at 0.1 MPa. It is considered that many

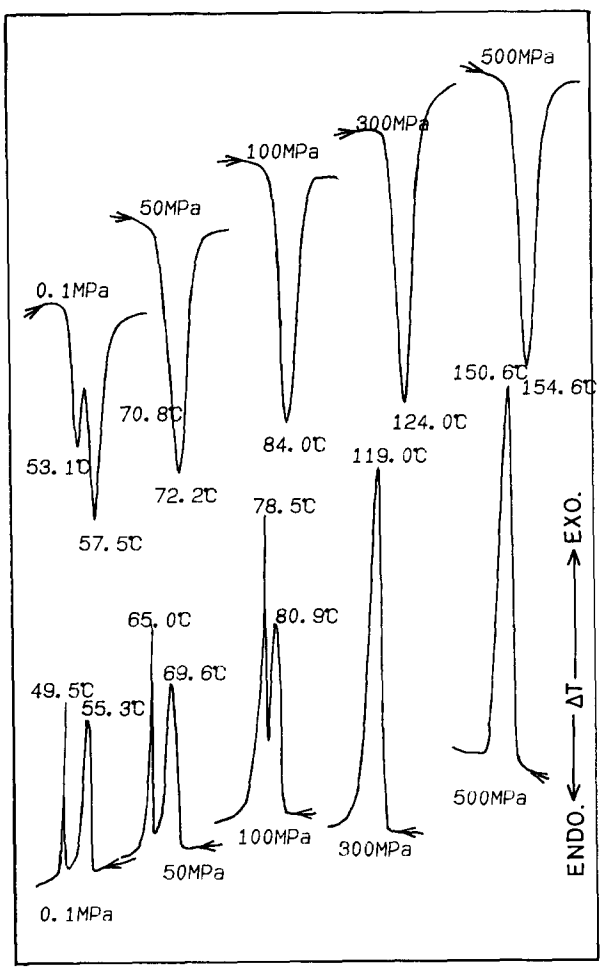

Figure 9 Effect of pressure on the d.t.a. melting and crystallization curves of pure C_{26}

Table 4 Values of A, B and C in the equation $T_h = A + BP - CP^2$, for the hexagonal transition temperature in the binary mixture of C_{30}/C_{26} for different weight fractions in d.t.a. up to 500 MPa

W_{C30}	A (°C)	B ($\times 10^{-1}$ K MPa^{-1})	C ($\times 10^{-4}$ K MPa^{-2})
1.0	63.4	3.38	3.282
0.9	58.6	2.80	1.408
0.8	57.3	2.74	1.501
0.6	51.4	2.65	1.439
0.5	48.9	2.51	1.167
0.4	47.8	2.65	1.449
0.2	46.7	2.54	1.223
0.1	44.4	2.52	1.198
0.0(C_{26})	51.9	3.39	3.312

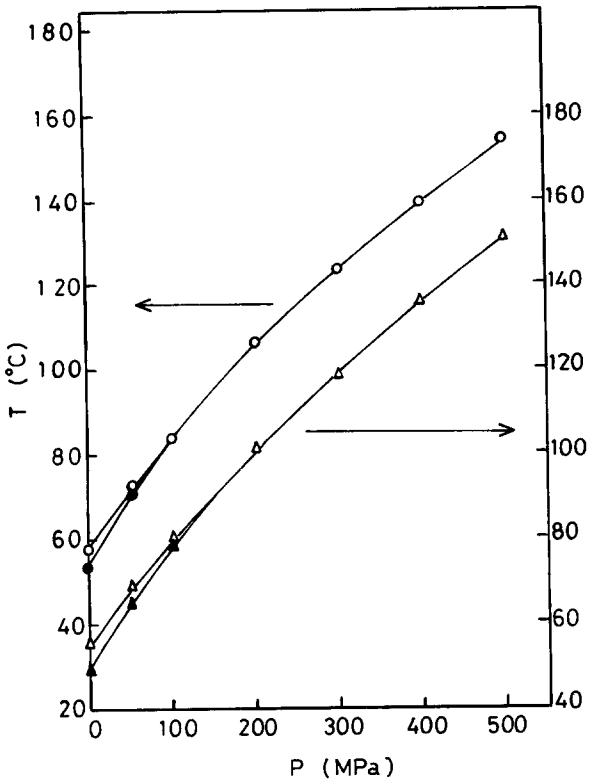

Figure 10 Pressure dependence of T_m and T_c of pure C_{26}. ○, T_m of C_{26}; ●, T_h in heating process; △, T_c of C_{26}; ▲, hexagonal–orthogonal transition in cooling process

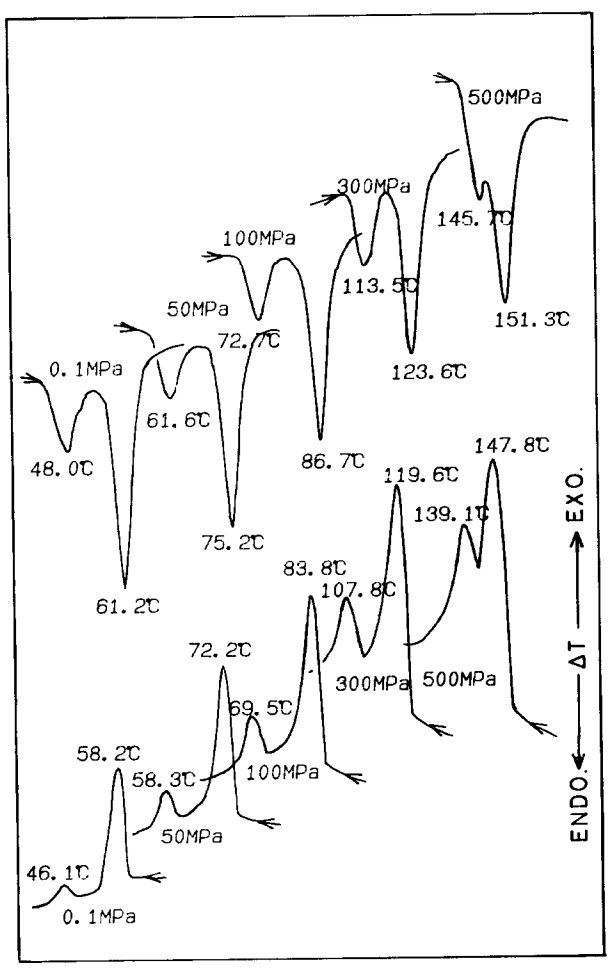

Figure 11 Effect of pressure on the d.t.a. melting and crystallization curves of the C_{30}/C_{26} mixture with $W_{C30}=0.5$

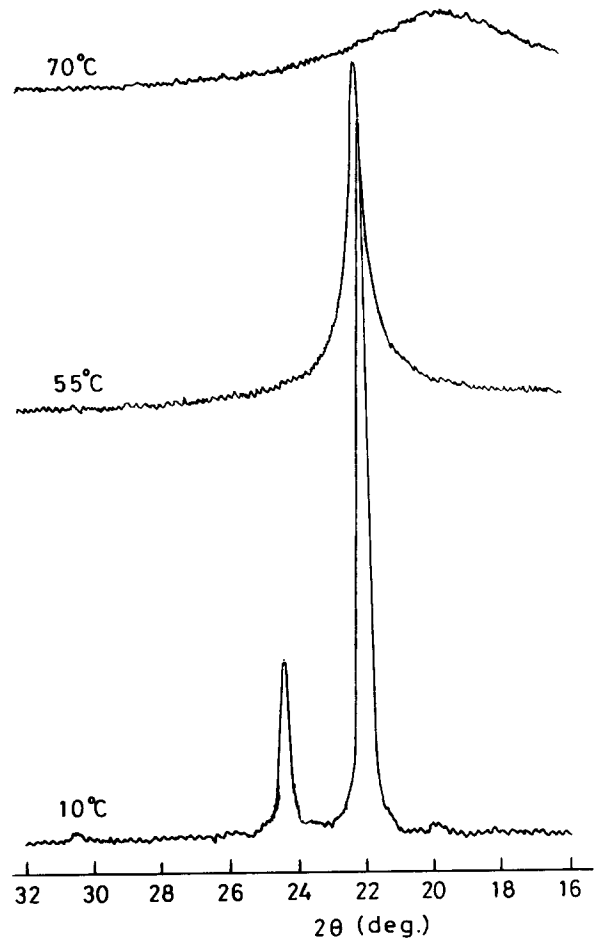

Figure 12 WAXD pattern of the C_{30}/C_{26} mixture with $W_{C30}=0.5$, at various temperatures

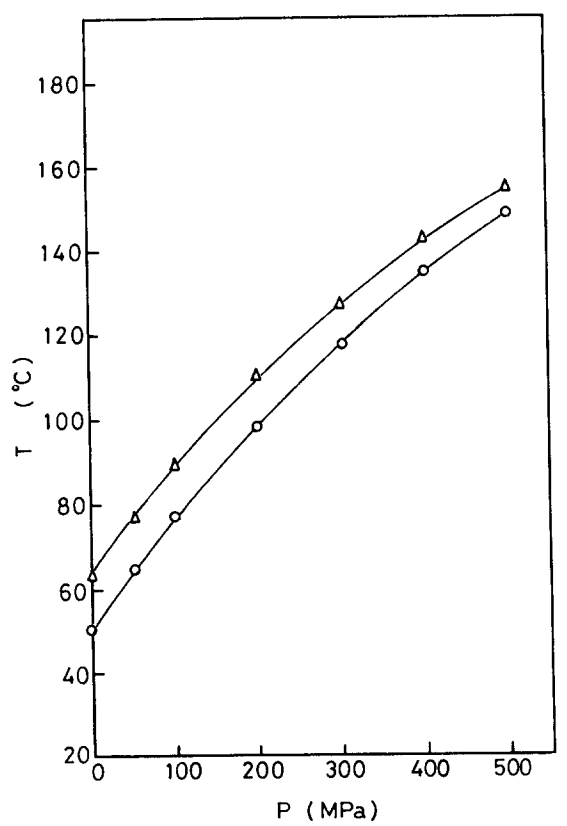

Figure 13 Pressure dependence of T_m (△) and T_h (○) of the C_{30}/C_{26} mixture with $W_{C30}=0.6$

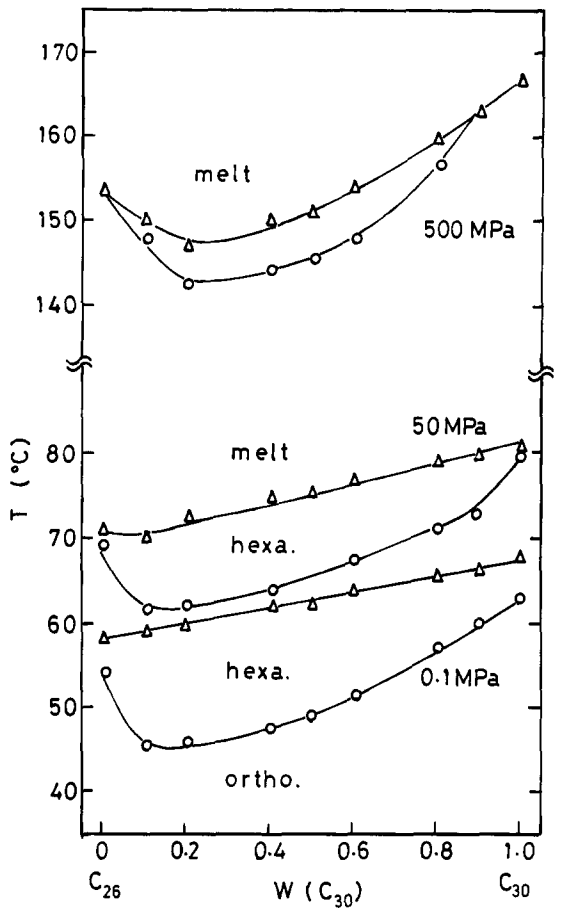

Figure 14 Phase diagram of the C_{30}/C_{26} mixture at various pressures (0.1, 50 and 500 MPa). ○, Hexagonal transition; △, melting of the hexagonal phase except for the pure C_{30} and C_{22} at high pressure and $W_{C30}=0.9$ at 500 MPa

molecular ends of C_{30} protrude from the crystal surface of the solid solution in this weight fraction, and the molecular motion of these free molecular ends becomes difficult at relatively lower temperature in the heating process. The fact that the longer chain n-alkane (C_{30}) is more effective in decreasing the transition temperature than the reverse case corresponds to the result reported for C_{22}/C_{19} (ref. 13). At elevated pressure, the temperature difference between T_m and T_h decreased and they merged above 100 MPa on both sides. At 500 MPa, this merging occurred at $W_{C30}=0.9$. In the phase diagram of the C_{21}/C_{19} binary mixture, the same merging occurred at 300 MPa in $W_{C21}=0.9$. The different behaviour of the phase diagrams of mixtures of C_{30}/C_{26} and C_{21}/C_{19} at elevated pressure should occur due to the different molecular length of the component alkanes. The difference in molecular length between C_{30} and C_{21} is 9 CH_2 units. The relative difference in molecular length between the component n-alkanes (4 CH_2 units for C_{30}/C_{26} and 2 CH_2 units for C_{21}/C_{19}) may not cause the different behaviour of the phase diagrams with change in pressure.

Under high pressure, above 100 MPa, the molecular motion of C_{30} is constrained and C_{30} crystals melt before the hexagonal transition. In $W_{C30}=0.9$, the number of defects should be smaller compared with the number in the medium region, so that the transition disappears. In the medium weight fraction, the hexagonal phase still appeared even at 500 MPa but at elevated pressure, above 500 MPa, the hexagonal phase may disappear.

CONCLUSION

The following conclusions can be drawn from this study on the melting and crystallization of C_{30}/C_{22} and C_{30}/C_{26} mixtures under high pressure.

The phase diagram of the binary mixture of C_{30}/C_{22} is eutectic due to the large difference of molecular length. The phase diagram changes at elevated pressure as follows. In the hyper-eutectic region on C_{30}, the hexagonal phase disappears above 100 MPa. The temperature difference between T_m of C_{30} and T_e increased with pressure. The pressure dependence of T_e is 0.247 K MPa^{-1}, which is smaller than that of T_m of pure C_{30} crystal (0.276 MPa^{-1}).

The binary mixture of C_{30}/C_{26} forms a solid solution. The phase diagram changes with pressure. A minimum appears at about $W_{C30}=0.2$ in the hexagonal transition curve, although the melting curve changes almost linearly from T_m of C_{22} to T_m of C_{30}. At elevated pressure, the melting curve becomes downwardly convex and the difference between the hexagonal transition curve and the T_m curve decreases. This is due to the decreased mobility of the molecules caused by the increased pressure.

REFERENCES

1 Wittmann, J. C. and Manley, R. St. J. *J. Polym. Sci., Polym. Phys. Edn* 1977, **15**, 2277
2 Smith, P. and Pennings, A. J. *Polymer* 1974, **15**, 413
3 Hodge, A. M., Kiss, G., Lotz, B. and Wittmann, J. C. *Polymer* 1982, **23**, 985
4 Vasanthakumari, R. *J. Macromol. Sci.-Chem.* 1983, **A20** (4), 463
5 Nakafuku, C. *Polym. J.* 1985, **17**, 869
6 Nakafuku, C. *Polymer* 1986, **27**, 353
7 Nechitailo, H. A., Tonchev, A. B., Rozenberg, P. M. and Terentueba, E. M. *J. Phys. Chem. USSR* (in Russian) 1960, **24**, 2694
8 Asbach, G. I., Kilian, H.-G. and Stracke, Fr. *Colloid Polym. Sci.* 1982, **260**, 151
9 Kilian, H.-G. *Makromol. Chem.* 1968, **116**, 219
10 Denicolo, I., Craievich, A. F. and Doucet, J. *J. Chem. Phys.* 1984, **80**, 6200
11 Dorset, D. L. *Macromolecules* 1986, **19**, 2965
12 Zhang, W. P. and Dorset, D. L. *J. Polym. Sci., Polym. Phys. Edn* 1990, **28**, 1223
13 Wurflinger, A. and Schneider, G. M. *Ber. Bunsenges. Phys. Chem.* 1973, **77**, 121
14 Takamizawa, K., Nagao, Y., Irii, D. and Urabe, Y. *Thermochim. Acta* 1985, **88**, 205
15 Richter, P. W. and Pistorius, C. W. F. T. *Mol. Cryst. Liq. Cryst.* 1972, **16**, 153
16 Takamizawa, K., Saida, S., Fujimoto, J., Urabe, Y. and Ogawa, Y. *Polym. Prepr. Jpn* 1991, **40**, 1152
17 Denicolo, I., Doucet, J. and Craievich, A. F. *J. Chem. Phys.* 1983, **78**, 1465
18 Nakafuku, C. *Polymer* 1981, **22**, 1963
19 Nakafuku, C., Nakagawa, H., Yasuniwa, M. and Tsubakihara, S. *Polymer* 1991, **32**, 696
20 Mazee, W. M. *Rec. Trav. Chim.* 1948, **67**, 197